PHYSICAL REVIEW B VOLUME 22, NUMBER 1 1 JULY 1980

Excitation spectrum and low-temperature thermodynamics of the Ising-Heisenberg linear ferromagnet

J. D. Johnson
Theoretical Division, Los Alamos Scientific Laboratory, Los Alamos, New Mexico 87545

J. C. Bonner
Physics Department, University of Rhode Island, Kingston, Rhode Island 02881
and Brookhaven National Laboratory, Upton, New York 11973
(Received 17 January 1980)

Important new analytic results have been obtained for the linear, ferromagnetic, spin-$\frac{1}{2}$, Ising-Heisenberg model in a small magnetic field. Specifically, for zero field an expression, which changes its form at an intermediate value of the variable anisotropy parameter, has been obtained for the thermal excitation energy gap. This special anisotropy value does not correspond to a symmetry change in the Hamiltonian, but is associated with an important difference in the physical significance of the results. For anisotropy greater than the special value, the dominant excitations correspond to bound spin complexes. For anisotropy less than the special value, the dominant excitations are spin waves. These results govern the low-temperature behavior of the specific heat. The effective magnetic excitation gap, which determines the low-temperature susceptibility, is dominated at zero field by the bound states for all anisotropy. More complex crossover effects occur in both specific heat and susceptibility when the analysis is extended to nonzero field. These results may have an important bearing on the quantum soliton problem in the linear ferromagnet.

I. INTRODUCTION

There has been a renewed surge of interest in exact solutions of nontrivial, quantum-mechanical, one-dimensional models.[1] For example, exact and fairly complete solutions are now available for the one-dimensional (1D), delta-function potential, Fermi and Bose gas models,[2–4] the linear Hubbard model of a metal-insulator transition,[5] and the linear, spin-$\frac{1}{2}$, Ising-Heisenberg-XY *continuum* model.[6] The method of solution of the linear magnetic continuum model is based on techniques for solving the 1D, field-theoretic, Tomonaga and Luttinger models.[7,8] These techniques have been further exploited in a somewhat different direction (incorporating the effects of spin and backward scattering) to obtain exact solutions for a continuum electron gas[9,10] and an electron gas on a lattice.[11,12] These are relevant to the important field of one-dimensional organic conductors.[13] Other interesting developments include exact treatments of the ground state of a 1D plasma with uniform background of opposite charge (which crystallizes as a Wigner solid)[14] and exact results for the Lai-Sutherland 1D model (which contains a dilute magnetic model and a generalized Hubbard model as special cases).[15] Models for organic charge transfer salts can be mapped into a quantum magnetic chain,[16,17] which in the antiferromagnetic limit corresponds to the Hubbard dimer gas.[18,19] At both zero[20] and finite[21,22] temperature one-dimensional quantum models of the general XYZ type can be mapped into 2D classical models. Analytic results for excitations of 1D quantum magnets in nonzero field[23–25] have yielded predictions of interesting new phenomena in spin dynamics.[25,26] Extensive application of exact solutions (solitons) of the 1D, quantum-mechanical, sine-Gordon, and related equations has been made to charge-density waves in 1D conductors.[11,12,27,28] Very recent use of exact Bethe's ansatz techniques has been made to solve the massive Thirring model.[29–31] Fadeev's review presents a unified approach to all the models discussed above.[30] Sutherland gives an overall view of the quantum soliton concept, together with new results for the quantization of the Toda lattice.[32]

Despite this flurry of activity, the solution for perhaps the best known model of all, the 1D, spin-$\frac{1}{2}$, Ising-Heisenberg-XY model, first studied in the 1930's[33,34] remains incomplete. The $T=0$ properties, including the critical singularities, are now known,[35] but the general solution is incomplete. By this we mean that for certain parameters ranges of the model the behaviors of the thermodynamic properties, the correlation functions, and the spectral excitations are not known. Specifically, exact information is lacking in the case of zero magnetic field on the anisotropic Ising-Heisenberg ferromagnet and the isotropic ferromagnet, and only partial information exists for the

isotropic antiferromagnet.

In this work we discuss interesting and rather complex results, which appear to be exact, for the elementary excitations and low-temperature thermodynamics of the spin-$\frac{1}{2}$, anisotropic, Ising-Heisenberg ferromagnet. Circumspection must be exercised in claiming an exact result for this fascinating but difficult problem because the form of solution depends crucially on the nature of a set of assumptions contained in the work of Gaudin.[36] Previous work of Johnson and McCoy[37] and Johnson[38] has resulted in additional analytical developments which have been used to extract finite-temperature results. When the results were compared with available numerical information,[38–40] a favorable comparison resulted, thus enhancing faith in the assumptions contained in the derivation of the formalism.

However, it is still worth emphasizing that there is no, *a priori,* obvious way to make the choice of assumptions, and, if a wrong choice is made, the analysis may be perfectly correct but the results will be meaningless.[41] Hence, it is valuable, even essential, to continue to compare the analytical answers with approximate but reasonably reliable alternative approaches, in this case perturbation theory and numerical studies on finite linear systems with both free-end and periodic boundary conditions.

For comparison with experimental magnetic systems, it is most convenient to express the Hamiltonian in the well-known form

$$H=-2J\sum_{i=1}^{N}[S_i^zS_{i+1}^z-\tfrac{1}{4}+\gamma(S_i^xS_{i+1}^x+S_i^yS_{i+1}^y)] \quad , \tag{1.1}$$

where γ is an anisotropy parameter which varies between the Ising model ($\gamma=0$) and the isotropic Heisenberg model ($\gamma=1$). Our studies show that a thermal energy gap exists for all $\gamma<1$, vanishing linearly as $1-\gamma$ as the isotropic limit is approached. Specifically, for $0\leq\gamma\leq 0.6$

$$\Delta E^{(1)}=\tfrac{1}{2}(E_i-E_0)=J(1-\gamma^2)^{1/2} \quad , \tag{1.2}$$

where the E_i are the dominant excited states and E_0 is the ferromagnetic ground state. For $0.6\leq\gamma<1$

$$\Delta E^{(2)}=2J(1-\gamma) \quad . \tag{1.3}$$

This crossover in behavior of the effective gap, midway through the anisotropy range, is rather surprising from smoothness-universality considerations. The principle involved is that the physical properties of a system should vary smoothly as a linear parameter in the Hamiltonian varies, provided that the underlying symmetry of the Hamiltonian remains unchanged.[42] There is no apparent symmetry change in the Hamiltonian at $\gamma=0.6$. However, on closer consideration, no obvious problem occurs, since ΔE is, in fact, continuous at $\gamma=0.6$. Further, the existence of a gap for all $\gamma<1$ implies exponential behavior of the thermodynamic functions as $T\to 0$ and identical (exponential) critical behavior at $T=0$.

Nevertheless, the behavior of the thermal excitation energy gap for the ferromagnet is different from the corresponding gap for antiferromagnets in that the antiferromagnetic gap is given by a *single*, albeit rather complicated, expression for all $0\leq\gamma\leq 1$. The formula may either be expressed as

$$\Delta E(\gamma)=\gamma|J|\sinh\Phi\sum_{n=-\infty}^{\infty}\frac{(-1)^n}{\cosh(n\Phi)} \quad , \tag{1.4}$$

which is suitable for numerical evaluation near the Ising limit, or as

$$\Delta E(\gamma)=\gamma\pi|J|\frac{\sinh\Phi}{\Phi}\sum_{n=-\infty}^{\infty}\frac{1}{\cosh[(n+\frac{1}{2})\pi^2/\Phi]} \quad , \tag{1.5}$$

which is more rapidly convergent near the Heisenberg limit. Here Φ is a convenient parameter such that $\cosh\Phi=1/\gamma$. Approximate forms of the expressions (1.4) and (1.5) are, for the Ising and Heisenberg limits, respectively,

$$\Delta E(\gamma)\simeq\begin{cases}|J|(1-2\gamma) & (1.6)\\ 4\pi\gamma|J|\exp\left[\dfrac{-\pi^2}{2}\left(\dfrac{\gamma}{2(1-\gamma)}\right)^{1/2}\right] \quad . & (1.7)\end{cases}$$

The antiferromagnetic energy gap is exactly half the gap obtained by des Cloizeaux and Gaudin from analytical studies on systems with periodic boundary conditions.[43]

For these reasons it is felt that the analytically predicted behavior of the anisotropic, ferromagnetic, thermal excitation gap is unusual enough to justify supporting studies by perturbation and other numerical methods. These backup studies not only make plausible the analytic result, but also are interesting in their own right, since they indicate clearly the nature of the different classes of low-lying excitations which are competing for dominance. Furthermore, these numerical studies are themselves, like the analytic approach, somewhat complicated, and may serve as a guide to the application of approximate theoretical procedures to problems for which an analytic solution is not, as yet, in sight, such as the alternating magnetic linear chain.

For $0\leq\gamma<0.6$ the dominant excitations are bound complexes of 2,3, . . . ,$\frac{1}{2}N$ neighboring spins, easily visualizable in the Ising limit. At low temperature they dominate both the susceptibility and the specific heat in the limit as the magnetic field tends to zero. The situation in the range $0.6<\gamma<1$ is more complex and therefore more interesting. The excitation energy gap of Eqs. (1.2) and (1.3) is actually the effective thermal excitation gap; i.e., it governs the low-temperature behavior of the specific

heat. In the range $0.6 < \gamma < 1$ spin-wave excitations dominate. The low-temperature behavior of the susceptibility, on the other hand, is governed over the *whole range of* γ, $0 \leq \gamma < 1$, by the bound-state gap, Eq. (1.2), which we may regard as the effective magnetic excitation gap. The unusual crossover effect noted above is thus seen to occur only for the thermal gap while the magnetic gap is given for all $0 \leq \gamma < 1$ by the bound-state expression. For finite magnetic field previous work[37] shows that the spin-wave states dominate both susceptibility and specific heat for all $0 \leq \gamma \leq 1$. Crossover effects abound, therefore, in the field-anisotropy parameter space, as will be discussed more specifically below. This complex behavior emphasizes the point that "standard spin-wave theory" may not correctly give even the leading terms of the low-temperature expansion.

An experimental demonstration of these excitation effects would be particularly challenging and interesting. Far-infrared absorption experiments, which reveal the dominance of bound-state excitations near the Ising limit, have already been carried out on the Ising-like linear chain $CoCl_2 \cdot 2H_2O$.[44] Resonance experiments and neutron scattering experiments might profitably be undertaken on $CoCl_2 \cdot 2(pyr)_2$, dichlorodipyridine cobalt (II), a better Ising-like linear chain than $CoCl_2 \cdot 2H_2O$. The recent discovery of a good Heisenberg-like linear ferromagnet[45] TMCuC (tetramethyl ammonium copper chloride) permits, in principle, experimental studies in the low anisotropy regime. However, quantum effects introduced by the strong transverse (XY) spin-coupling terms may cause some difficulty in distinguishing between classes of bound and spin-wave states.

In Sec. II of the paper the analytic results will be presented, and in Sec. III the supporting numerical studies will be discussed. Conclusions are drawn and a final discussion is given in Sec. IV.

II. ANALYTIC APPROACH

In this section the Gaudin[36] free-energy expression is discussed and a complete solution is then given for zero field in the form of a low-temperature expansion, paying careful attention to error terms at every stage. The results are then generalized to small finite field. It is then shown how simplified spin-wave-type arguments may be used to derive the same results more easily. Finally, a detailed discussion is given of the behavior of the susceptibility and specific heat in various regions of the field-anisotropy parameter space.

The Hamiltonian (1.1), which is convenient for numerical studies and comparison with experiment, is not appropriate for exact analytic work. Hence, we use the following form of the Ising-Heisenberg Hamiltonian in a field

$$H = -\sum_{i=1}^{N} [S_i^x S_{i+1}^x + S_i^y S_{i+1}^y + \Delta(S_i^z S_{i+1}^z - \tfrac{1}{4})] - H_0 \sum_{i=1}^{N} S_i^z \ . \tag{2.1}$$

This may be compared with Eq. (1.1) in which a Zeeman term $-g\beta H_M \sum_{i=1}^{N} S_i^z$ has been added. In what follows, therefore, $\Delta = \gamma^{-1}$, $T = k_B T_P/(2\gamma J)$, and $H_0 = g\beta H_M/(2\gamma J)$. T_P is the physical temperature and k_B is Boltzmann's constant.

A. Formalism of Gaudin for $H_0 = 0$ and $\Delta > 1$

Gaudin[36] has obtained the following expression for the free energy per site:

$$F(T) = -E_0(\Delta) - \frac{T}{2\pi} \int_{-\pi}^{\pi} \mathrm{Dn}(\phi) \ln(1 + e^{\epsilon_1(\phi)/T}) d\phi \ , \tag{2.2}$$

where $E_0(\Delta)$ is the antiferromagnetic ground-state energy when $\Delta = -\Delta$.[46] The known function, $\mathrm{Dn}(\phi)$, is defined as

$$\mathrm{Dn}(\phi) = (K_k/\pi)\, \mathrm{dn}(K_k \phi/\pi, k) \ , \tag{2.3a}$$

where K_k is the complete elliptic integral of the first kind and $\mathrm{dn}(\phi, k)$ is one of the Jacobian elliptic functions.[47] The modulus k of these functions is given by

$$K_{k'}/K_k = \Phi/\pi \ , \tag{2.3b}$$

where $k' = (1 - k^2)^{1/2}$. Explicitly,

$$E_0(\Delta) = -\frac{\sinh\Phi}{2\pi} \int_{-\pi}^{\pi} \frac{\mathrm{Dn}(\phi) \sinh\Phi}{\cosh\Phi - \cos\phi} d\phi \ . \tag{2.4}$$

For the antiferromagnet, when $T \to 0$, the integral in Eq. (2.2) vanishes, whereas for the ferromagnet, when $T \to 0$, the integral cancels with $E_0(\Delta)$ to give zero (independent of Δ). This is, of course, the ferromagnetic ground state for our Hamiltonian (2.1).

Clearly, to determine the low-temperature excitations, we must find an expression for the function $\epsilon_1(\phi)$. For this we must solve an infinite set of coupled, nonlinear, integral equations; namely,

$$\epsilon_1(\phi) = \frac{T}{2\pi} \int_{-\pi}^{\pi} \mathrm{Dn}(\phi - \phi') \ln(1 + e^{\epsilon_2(\phi')/T}) d\phi' + \sinh\Phi\, \mathrm{Dn}(\phi) \tag{2.5a}$$

and

$$\epsilon_n(\phi) = \frac{T}{2\pi} \int_{-\pi}^{\pi} \mathrm{Dn}(\phi - \phi') \ln(1 + e^{\epsilon_{n+1}(\phi')/T}) \times (1 + e^{\epsilon_{n-1}(\phi')/T}) d\phi', \quad n \geq 2 \ . \tag{2.5b}$$

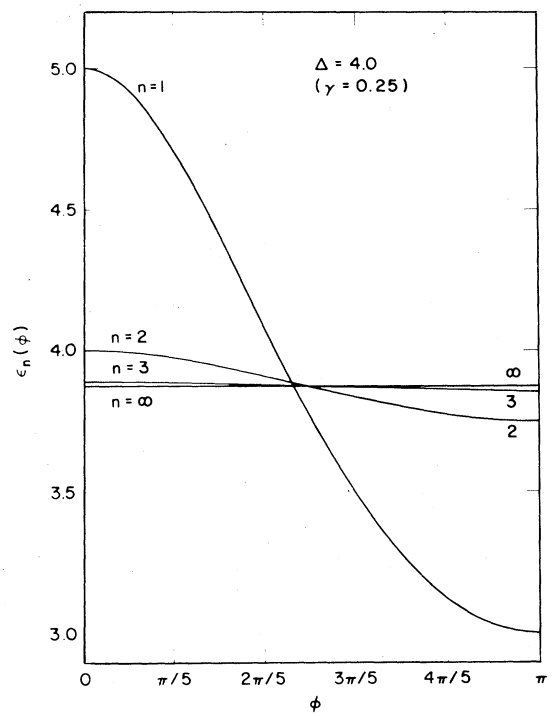

FIG. 1. Plot of the $\epsilon_n(\phi)$ for $T=0$ and large anisotropy, $\Delta=4.0(\gamma=0.25)$.

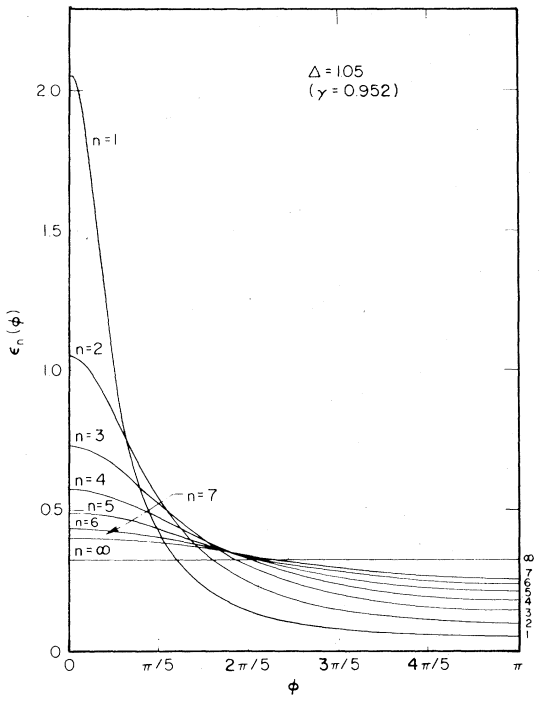

FIG. 2. Plot of the $\epsilon_n(\phi)$ for $T=0$ and small anisotropy, $\Delta=1.05(\gamma=0.952)$.

The set of equations for the $\epsilon_n(\phi)$ is completed with a boundary condition $\lim_{n\to\infty}\epsilon_n(\phi)/n=0$. Equations (2.2) through (2.5) completely determine the free energy $F(T)$, which may then be differentiated to obtain the entropy, S, and constant field specific heat, C_H, per spin.

To give the reader some idea of the behavior of the $\epsilon_n(\phi)$, we present in Figs. 1 and 2 the zero temperature $\epsilon_n(\phi)$, $n=1,2,3,\ldots,\infty$, for $\Delta=4.0$ and 1.05. A point to note is that, as n increases, the $\epsilon_n(\phi)$ goes to a constant independent of both n and ϕ. We describe this effect, for n large, as "saturation." As we go from large Δ to $\Delta\simeq 1$, the value of n at which the curves saturate goes from a rather low value to much larger values. We shall see later that this saturation phenomenon, in particular the ϕ independence, is an important ingredient in extracting an exact solution. Lack of saturation near $\Delta=1$ is one reason why our analysis cannot be extended to this important limit. Finally, we note that the $\epsilon_n(\phi)$ are not energy dispersion curves, although they are related to them.[38]

In what follows we require what we term the "Ising solution" of Eqs. (2.5), which plays the vital role of putting bounds on the $\epsilon_n(\phi)$. If the driving term of Eq. (2.5a) is replaced by a ϕ-independent term $\frac{1}{2}DT$, the equations can be solved analytically. The solution is

$$\epsilon_n^I = T\ln[(e^{D/2}+n)^2-1], \quad n\geq 1 \ . \tag{2.6}$$

If $D=2\sinh\Phi\{(\max,\min)[\mathrm{Dn}(\phi)]\}/T$, the resulting ϵ_n^I give (*upper, lower*) bounds on the $\epsilon_n(\phi)$. Furthermore, if, at some $n=n_0$, $\epsilon_{n_0}^I$ is chosen to bound $\epsilon_{n_0}(\phi)$ below (above), then the $\epsilon_n^I, n\geq n_0$, also bound the $\epsilon_n(\phi)$, $n\geq n_0$, below (above).[38] These bounding properties of the ϵ_n^I imply that

$$0<\min\epsilon_1(\phi)<\min\epsilon_2(\phi)<\cdots<\min\epsilon_l(\phi)<\min\epsilon_{l+1}(\phi)<\cdots \tag{2.7}$$

B. Low-temperature expansion for $H_0=0$ and $\Delta>1$

It is useful, for the sake of conciseness in the following work, to define

$$\eta_n(\phi)=\ln(1+e^{-\epsilon_n(\phi)/T}) \tag{2.8a}$$

and

$$g_n(\phi)=\sinh(n\Phi)/[\cosh(n\Phi)-\cos\phi] \ . \tag{2.8b}$$

Since error estimates are an important feature, it is useful to define error terms

$$\delta_n=O(T^b e^{-c/T}e^{-\min\epsilon_n(\phi)/T}) \ , \tag{2.8c}$$

where b is a number, not large (say less than 10) in absolute value, and $c \geq 0$. We also need

$$\delta(a) = O(T^b e^{-a/T}) \ , \tag{2.8d}$$

where again $a \geq 0$ and b is not large. In what follows, a, b, and c are used, as above, to denote numbers defined only for the equation of interest. (b and c, in fact, can have different values within the same equation.) Throughout this paper, a, b, and c are always independent of T.

We now rewrite Eqs. (2.5) in terms of infinite sums. It is convenient to manipulate Eq. (2.5) in this way for reasons which become clear later in a discussion of the saturation property of the $\epsilon_n(\phi)$. Specifically, we take the $\exp[\epsilon_n(\phi)/T]$ out of the ln terms on the right-hand side (RHS) of Eq. (2.5) and eventually solve the resulting equations treating the nonlinear parts as known functions. The equations remain exact at this point.

$$\epsilon_1(\phi) = \sinh(\Phi) g_1(\phi) + \frac{T}{2\pi} \int_{-\pi}^{\pi} g_2(\phi - \phi') \eta_1(\phi') d\phi' + \frac{T}{\pi} \sum_{l=2}^{\infty} \int_{-\pi}^{\pi} \eta_l(\phi') d\phi'$$
$$+ \frac{T}{2\pi} \sum_{l=2}^{\infty} \int_{-\pi}^{\pi} [g_{l-1}(\phi - \phi') + g_{l+1}(\phi - \phi') - 2] \eta_l(\phi') d\phi' \ . \tag{2.9}$$

The last term of Eq. (2.9) is δ_2, uniformly in ϕ. Hence,

$$\epsilon_1(\phi) = \sinh(\Phi) g_1(\phi) + \frac{T}{2\pi} \int_{-\pi}^{\pi} g_2(\phi - \phi') \eta_1(\phi') d\phi' + \frac{T}{\pi} \sum_{l=2}^{\infty} \int_{-\pi}^{\pi} \eta_l(\phi') d\phi' + \delta_2 \ . \tag{2.10a}$$

The surviving infinite sum is the term which causes difficulty and which we subseqently must estimate. Similarly for $n \geq 2$

$$\epsilon_n(\phi) = \sinh(\Phi) g_n(\phi) + \frac{T}{2\pi} \int_{-\pi}^{\pi} [g_{n+1}(\phi - \phi') + g_{n-1}(\phi - \phi') - 2] \eta_1(\phi') d\phi'$$
$$+ \frac{T}{2\pi} \sum_{l=1}^{\infty} (l + n - |l - n| - \delta_{l,n}) \int_{-\pi}^{\pi} \eta_l(\phi') d\phi' + \delta_2 \ , \tag{2.10b}$$

where δ_2 is uniformly good in ϕ and n. The terms appearing as the infinite sums in Eqs. (2.10) will henceforth be denoted the Ω_n terms; i.e.,

$$\Omega_1 = \frac{T}{\pi} \sum_{l=2}^{\infty} \int_{-\pi}^{\pi} \eta_l(\phi') d\phi' , \tag{2.11a}$$

$$\Omega_n = \frac{T}{2\pi} \sum_{l=1}^{\infty} (l + n - |l - n| - \delta_{l,n}) \int_{-\pi}^{\pi} \eta_l(\phi') d\phi' , \quad n \neq 1 \ . \tag{2.11b}$$

Bounding the $\epsilon_n(\phi)$ with Ising solutions, we can show for *fixed* n, that the Ω_n terms are exponentially small in T. Therefore, for *fixed* n, $\epsilon_n(\phi) = \sinh(\Phi) g_n(\phi) + \delta(a), n \geq 1, a > 0$. In previous work, when the external magnetic field H_0 was not zero,[37] the Ω_n sums converged quite rapidly because the $\epsilon_n(\phi)$ contained a term nH_0. Now, for large n it appears that the $\epsilon_n(\phi)$ saturate, as discussed above, and one might naively conclude that the Ω_n sums do not converge. The correct picture, however, is that one must estimate the Ω_n sums for small T and *all* n (uniformly in n). We find for T small, but fixed, that as $n \to \infty$ the Ω_n sums do diverge, which implies that the $\epsilon_n(\phi)$ do not saturate. In fact, for large n and small, but fixed, T, $\epsilon_n(\phi) = 2T \ln(n) +$ corrections. This allows the Ω_n terms to exist for fixed n. Finally, in previous work with $H_0 \neq 0$ it was found that Ω_1 was bounded by δ_2 and could be neglected. This is again the result of the nH_0 term in $\epsilon_n(\phi)$. For $H_0 = 0$ we can no longer neglect Ω_1, and it is not immediately clear what is the order in T of Ω_1. Hence, the main problem we now face is to estimate Ω_1. The details will be quite complicated since obviously a careful analysis of error terms is necessary. The reader interested mainly in our principal results may wish to skip to Eq. (2.17) towards the end of this subsection.

We choose an n_0 of order $O(\min\epsilon_3(\phi)/\Phi T)$ and define $\epsilon_n^c = \sinh\Phi + \Omega_n$. We define ϵ_n^d such that, at $n = n_0$, $\epsilon_{n_0}^d = \epsilon_{n_0}^c$, and for $n > n_0$ the ϵ_n^d are Ising solutions to the $\epsilon_n(\phi)$ equations. That is, the ϵ_n^d are the same as the ϵ_n^I in subsection II A with the D term so chosen that $\epsilon_{n_0}^I = \epsilon_{n_0}^d = \epsilon_{n_0}^c$; the ϵ_n^d are a specific ϵ_n^I. Using the Ising upper and lower bounds, we can show that $\epsilon_n^c = \epsilon_n^d + \delta_2$, $n \geq n_0$, and $\epsilon_n(\phi) = \epsilon_n^c + \delta_2$, $n \geq n_0$. We know the ϵ_n^d exactly:

$$\epsilon_n^d = T \ln[(e^{D_{n_0}/2} + n - n_0)^2 - 1], \quad n > n_0 \ , \tag{2.12}$$

where $D_{n_0} = \ln[1 + \exp(\epsilon_{n_0}^c/T)]$.

In Ω_1 we drop the sum from $l = 2$ to $n_0 - 1$ with an error δ_2. Since $\epsilon_n(\phi) = \epsilon_n^d + \delta_2$, $n \geq n_0$, we can ap-

proximate the rest of Ω_1 to obtain

$$\epsilon_1(\phi)=\sinh(\Phi)g_1(\phi)+\frac{T}{2\pi}\int_{-\pi}^{\pi}g_2(\phi-\phi')\eta_1(\phi')d\phi'+2T\sum_{l=n_0}^{\infty}\ln(1+e^{-\epsilon_l^d/T})+\delta_2 \quad (2.13)$$

The sum can be performed to yield

$$\epsilon_1(\phi)=\sinh(\Phi)g_1(\phi)+\frac{T}{2\pi}\int_{-\pi}^{\pi}g_2(\phi-\phi')\eta_1(\phi')d\phi'+2T\ln(1+e^{-D_{n_0}/2})+\delta_2 \quad (2.14)$$

To find D_{n_0}, we take $\epsilon_n^c=\sinh\Phi+\Omega_n$ with $n=n_0$ and analyze the infinite sum Ω_{n_0} in the same way as we have just treated Ω_1. We obtain

$$\epsilon_{n_0}^c=\sinh\Phi+2n_0T\ln(1+e^{-D_{n_0}/2})+\delta(a)+\delta_1, \quad (2.15)$$

$a>TD_{n_0}/2$. By definition $D_{n_0}=\epsilon_{n_0}^c/T+\ln(1+e^{-\epsilon_{n_0}^c/T})$. Therefore,

$$\epsilon_{n_0}^c=\sinh\Phi+2n_0Te^{-\sinh(\Phi)/(2T)}+\delta(a)+\delta_1 , \quad (2.16)$$

$a>\frac{1}{2}\sinh\Phi$. Hence,

$$\epsilon_1(\phi)=\sinh(\Phi)g_1(\phi)+\frac{T}{2\pi}\int_{-\pi}^{\pi}g_2(\phi-\phi')\ln(1+e^{-\epsilon_1^0(\phi')/T})d\phi'+2Te^{-\sinh(\Phi)/(2T)}+\delta_2+\delta_1^2+\delta_1O(e^{-\sinh(\Phi)/(2T)})+\delta(a) , \quad (2.17)$$

where $\epsilon_1^0(\phi)=\sinh(\Phi)g_1(\phi)$ and $a=\sinh\Phi$. From Eq. (2.2)

$$F(T)=\frac{\sinh\Phi}{2\pi}\int_{-\pi}^{\pi}\mathrm{Dn}(\phi)g_1(\phi)d\phi-\frac{T}{2\pi}\int_{-\pi}^{\pi}\mathrm{Dn}(\phi)\ln(1+e^{\epsilon_1(\phi)/T})d\phi . \quad (2.18)$$

We now substitute Eq. (2.17) into Eq. (2.18) to obtain

$$F(T)=-Te^{-\sinh(\Phi)/(2T)}-\frac{T}{2\pi}\int_{-\pi}^{\pi}d\phi g_1(\phi)e^{-\sinh(\Phi)g_1(\phi)/T}+\delta(a) , \quad (2.19)$$

where $a>\min[\frac{1}{2}\sinh\Phi, \sinh(\Phi)g_1(\pi)]$. If we define $q=\int_0^{\phi}g_1(\phi')d\phi'+\pi$, then

$$F(T)=-Te^{-(\Delta^2-1)^{1/2}/(2T)}-\frac{T}{2\pi}\int_0^{2\pi}dqe^{-(\Delta-\cos q)/T}+\delta(a) , \quad (2.20)$$

where $a>\min[(\Delta^2-1)^{1/2}/2, \Delta-1]$ and $\Delta>1$. Δ is fixed as $T\to 0$. This is our zero-field result.

C. Extension to small finite field and $\Delta>1$

The work just presented can be generalized to small, but finite, H_0. The generalization is straightforward, but even more lengthy, and, hence, we shall just present results. For $0\le H_0<O(T^{\zeta})$, $\zeta>0$ and independent of T, but excluding a small $O(T^0)$ neighborhood of $H_0=O, \Delta=1$, we have

$$F(T,\sigma)-\sigma H_0=-\{H_0^2/4+T^2\exp[-(\Delta^2-1)^{1/2}/T]\}^{1/2}-\frac{T}{2\pi}\int_0^{2\pi}dqe^{-(\Delta+H_0-\cos q)/T}+\cdots , \quad (2.21)$$

where the ellipses represent correction terms. σ is the magnetization per spin. The corrections are such that one can treat the two terms on the RHS of Eq. (2.21) as an exact expression for any number of T derivatives (including zero) and up to and including two H_0 derivatives. The error in the answer will be exponentially smaller (higher order) in T than the leading order; i.e., the error is $\delta(a)$, $a>0$, times the leading-order term. For $H_0>O(T^{\zeta})$, $\zeta>0$, replace the first term on the RHS of Eq. (2.21) by $-H_0/2$. The correction is exponentially higher order in T than the integral. This result for $H_0>O(T^{\zeta})$ merges smoothly onto the $H_0<O(T^{\zeta})$ result and contains no interesting structure. Therefore, for the remainder of the paper we restrict $\Delta>1$ and $0\le H_0<O(T^{\zeta})$, $\zeta>0$. Δ and ζ are always fixed as $T\to 0$. Thus, we now have a complete study of the low-temperature thermodynamics of the ferromagnetic Ising-Heisenberg model with the exception of a small $O(T^0)$ neighborhood of $H_0=0, \Delta=1$.

Low-temperature expansions have been done by Takahashi[48] on the $H_0=0$ XYZ model. These calculations are easier in that contributions from only a finite number of $\epsilon_n(\phi)$ are required. Therefore, as Takahashi notes, his analysis is not valid when the XYZ Hamiltonian is specialized to Eq. (2.1) with $H_0=0$. It is interesting that, if one, nevertheless, ex-

amines the Takahashi low-temperature thermodynamics in this limit, the answer is the same as our Eq. (2.20). Therefore, we now have a complete picture of the $H_0 = XYZ$ model at low-temperature, except for the neighborhood of $\Delta = 1$ (Heisenberg limit) and possibly for the Heisenberg-XY line, $1 > \Delta > 0$. However, the field-dependent free energy and susceptibility equations cannot be obtained from Takahashi's work since the $H_0 \neq 0$ XYZ model has not been solved.

D. Simplified approach

In order to illustrate some of the physics of our result, we present a simple spin-wave type of argument. The calculation is good for $0 \leq H_0 < O(T^\zeta)$, $\zeta > 0$, with $\Delta > 1$.

For $T = 0$ the elementary excitations are given by

$$E_n(P) = nH_0 + \sinh\Phi[\cosh(n\Phi) - \cos P]/\sinh(n\Phi) \ , \tag{2.22}$$

where $n = 1, 2, 3, \ldots$, and $0 \leq P \leq 2\pi$.[37,38] The P's are distributed uniformly between 0 and 2π and, for a given n, obey a Fermi-like exclusion principle. The energies of the first excited states are $E_1(q) = H_0 + \Delta - \cos q$. There are N such states with $q = 2\pi n/N$, $0 \leq q \leq 2\pi$. The states we first sum up are these N states, the $\frac{1}{2}N(N-1)$ states with energies $E_1(q_1) + E_1(q_2), \ldots$, the $N!/[l!N-l)!]$ states with energies $E_1(q_1) + E_1(q_2) + \cdots + E_1(q_l)$, etc. These are all the $n = 1$ excitations with no higher n excitations. They provide a contribution to $F(T, \sigma)$ (Ref. 37) of

$$F(T, \sigma) = \sigma H_0 - \frac{T}{2\pi}\int_0^{2\pi} dq e^{-(H_0+\Delta-\cos q)/T} \ . \tag{2.23}$$

We now sum out the high-n excitations. Intuition suggests that these excitations could be important for small H_0 since for $H_0 = 0$ the $E_n(P)$ saturate to a constant for large n. For large n, $E_n(P) \sim nH_0 + \sinh\Phi$; i.e., $E_n(P)$ is independent of P. In fact, these energies are just those of a one-dimensional Ising model whose exchange constant $J = \sinh\Phi$. Accordingly, we add to Eq. (2.23) the Ising free energy[49] for this J. We obtain

$$F(T, \sigma) = \sigma H_0 - \frac{T}{2\pi}\int_0^{2\pi} dq e^{-(H_0+\Delta-\cos q)/T} - T\ln\{\cosh(H_0/2T) + [\cosh^2(H_0/2T) - 2e^{-\sinh(\Phi)/(2T)}\sinh(\sinh\Phi/2T)]^{1/2}\} \ . \tag{2.24}$$

If we expand Eq. (2.24) for low T, we obtain Eq. (2.21). Thus we have learned that the two principal contributions to the low-temperature thermodynamics are from the $n = 1$ excitations and the high-n, Ising-like, excitations.

E. Discussion of χ and C_H

Equation (2.21) may be differentiated to yield the specific heat, C_H, and the susceptibility, χ. The susceptibility for $0 \leq H_0 < O(T^\zeta)$, $\zeta > 0$, with $\Delta > 1$ is given by

$$\chi = T^2 e^{-(\Delta^2-1)^{1/2}/T}[4(H_0^2/4 + T^2 e^{-(\Delta^2-1)^{1/2}/T})^{3/2}]^{-1} + (2\pi T)^{-1}\int_0^{2\pi} dq e^{-(\Delta+H_0-\cos q)/T} + \cdots \ , \tag{2.25}$$

where the ellipses again represent correction terms. The corrections are exponentially higher order in T than the larger of the two terms displayed in Eq. (2.25). The integral can be expanded to give

$$\chi = T^2 e^{-(\Delta^2-1)^{1/2}/T}[4(H_0^2/4 + T^2 e^{-(\Delta^2-1)^{1/2}/T})^{3/2}]^{-1} + (2\pi T)^{-1/2} e^{-(\Delta+H_0-1)/T} + \cdots \ . \tag{2.26}$$

Similarly, for the specific heat, again for $0 \leq H_0 < O(T^\zeta)$, $\zeta > 0$, with $\Delta > 1$,

$$C_H = (2\pi T^3)^{-1/2}(\Delta + H_0 - 1)^2 e^{-(\Delta+H_0-1)/T} + (\Delta^2-1)e^{-(\Delta^2-1)^{1/2}/T}(H_0^2/2 + T^2 e^{-(\Delta^2-1)^{1/2}/T}) \times [4T(H_0^2/4 + T^2 e^{-(\Delta^2-1)^{1/2}/T})^{3/2}]^{-1} + \cdots \ . \tag{2.27}$$

The ellipses again represent corrections. The corrections to χ are exponentially higher order in T than the first term of χ and $O(T)$ higher order than the second term (order T times the second term). The corrections to C_H are $O(T)$ higher order than the larger of the two terms of C_H.

Let us discuss χ. It is convenient to change variables from H_0 to α so that $H_0 = e^{\alpha/T}$. The dominant behavior of χ varies in different regions of $\alpha - \Delta$ space, as shown in Fig. 3(a). For $\alpha > \alpha_b = \frac{1}{3}[\Delta - 1 - (\Delta^2-1)^{1/2}]$, the second term of expression (2.25) for χ (the spin-wave term) dominates the first term (the bound-state term). For $\alpha < \alpha_b$ the bound states dominate χ. The bound-state region, however, subdivides into two qualitatively different regions. For $\alpha < \alpha_c = -\frac{1}{2}(\Delta^2-1)^{1/2}$, the $\frac{1}{4}H_0^2$ term in the denominator can be dropped, to exponential accuracy, i.e., the error is exponentially higher order in T,

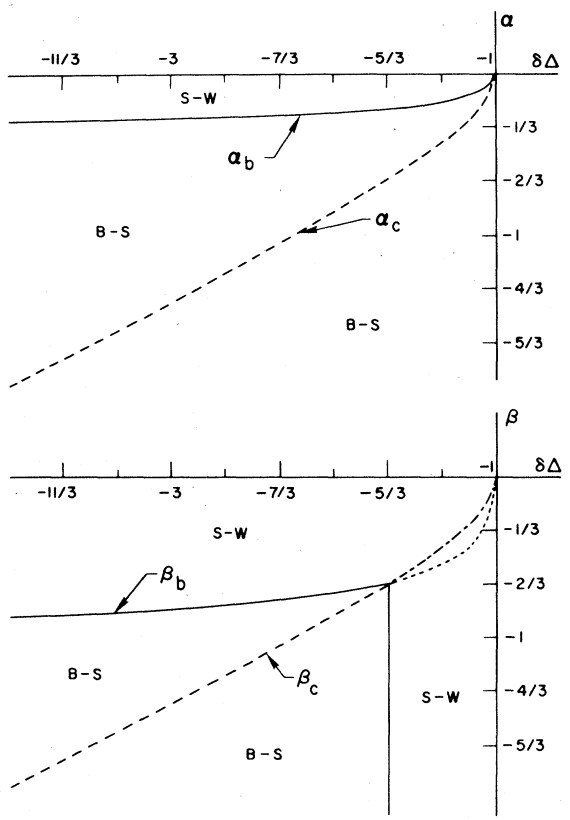

FIG. 3. (a) Nature of the various regions and corresponding crossover boundaries which determine the low-temperature behavior of the susceptibility as a function of field $\alpha(=T\ln H_0)$ and anisotropy $\delta\Delta$. $\delta=-1$ in this figure, and $\Delta>1$ is our region of interest. (b) Corresponding figure for the low-temperature specific heat. $(\beta=T\ln H_0.)$

to obtain

$$\chi=(4T)^{-1}e^{(\Delta^2-1)^{1/2}/(2T)} \quad . \tag{2.28}$$

This gives χ in the neighborhood of the $H_0=0$ peak. The region in the neighborhood of $\alpha=\alpha_c$ is a crossover region in H_0, where one cannot simplify the first term of Eq. (2.25). However, for $\alpha_b>\alpha>\alpha_c$ we can again simplify the expression for χ to obtain

$$\chi=2T^2H_0^{-3}e^{-(\Delta^2-1)^{1/2}/T} \quad . \tag{2.29}$$

This expression, again, is exponentially accurate in T.

For C_H we proceed in a similar manner by defining $H_0=e^{\beta/T}$. Again, different types of behavior dominate in the $\beta-\Delta$ plane, as sketched in Fig. 3(b). For $\Delta<\frac{5}{3}$ and all $\beta(H_0)$, the first term of Eq. (2.27) dominates; i.e., the specific heat is completely determined by the spin-wave states. For $\Delta>\frac{5}{3}$, however, we have a spin-wave-dominated region and a bound state [second term of Eq. (2.27)] dominated region. Specifically, for $\beta>\beta_b=\Delta-1-(\Delta^2-1)^{1/2}$ and $\Delta>\frac{5}{3}$, the spin-waves dominate, while for $\beta<\beta_b$, $\Delta>\frac{5}{3}$, the bound-states dominate. As in the case of the susceptibility, the bound-state region subdivides. For $\beta<\beta_c=-(\Delta^2-1)^{1/2}/2$, the H_0 terms of C_H [Eq. (2.27)] can be dropped to give

$$C_H=(\Delta^2-1)e^{-(\Delta^2-1)/(2T)}(4T^2)^{-1} \quad . \tag{2.30}$$

The corrections are $O(T)$ higher order. At $\beta=\beta_c$ we pass through a crossover region in which the whole second term of Eq. (2.27) must be used. For $\beta_b>\beta>\beta_c$ we can approximate C_H as

$$C_H=(\Delta^2-1)e^{-(\Delta^2-1)^{1/2}/T}(TH_0)^{-1} \quad , \tag{2.31}$$

with corrections $O(T)$ higher order.

Thus, for the ferromagnetic Ising-Heisenberg model, we have a rather complicated picture in the neighborhood of zero field. There are several regions in $H_0-\Delta$ parameter space which have qualitatively different low-temperature thermodynamics with crossover behavior between regions. The types of excitation that give rise to the low-temperature behavior change from region to region. Further, we note with interest that the qualitative picture for the susceptibility is not the same as for the specific heat.

III. NUMERICAL STUDIES FOR ZERO FIELD

A. Effective gap: Rings versus chains

In this subsection we shall compare the spectral properties of finite linear magnetic systems with periodic (rings) and free-ended (chains) boundary conditions. In the Ising limit, which is easily accessible, we shall discuss an interesting feature of the energy spectrum which differs in the two cases. This feature is fairly well known (at least in the Ising limit). Our reason for emphasizing it here is that conclusions based on it appear to have validity also for the zero-field $(H_0=0)$ Ising-Heisenberg problem $(|\Delta|>1)$.

At the Ising limit the chain levels form a significantly different pattern from the rings; i.e., levels appear at $E=0, |J|, 2|J|, 3|J|, \ldots, (N-1)|J|$, rather than just for $E=0, 2|J|, 4|J|, \ldots$, as for rings. The first excited ferromagnetic Ising level for chains at $|J|$ contains $4(N/2-1)+2=2N-2$ states, which may be regarded as having split off the ring level at $2|J|$ under the influence of a perturbation arising from the change of boundary conditions. The degeneracy of the second excited chain level is then $N(N-1)-2(N-1)$, i.e., is still $O(N^2)$. Since this dissimilarity persists to the limit $N=\infty$, it might appear that finite rings and chains predict different limiting behavior for the spectrum; in particular, for the effective energy gap ΔE between the ground and ex-

cited states. To understand why this does not occur, we look at the exact solution for the partition function Z_n for finite rings and chains, respectively,

$$Z_N = \begin{cases} (2e^{-J/2k_BT_P})^N[\cosh^N(J/2k_BT_P) \\ \qquad +\sinh^N(J/2k_BT_P)] & (3.1) \\ (2e^{-J/2k_BT_P})^N[\cosh(J/2k_BT_P)]^{N-1}. & (3.2) \end{cases}$$

One may see from a series expansion of Eqs. (3.1) and (3.2) that there is an "accidental" canceling of the odd powers of exp $(-J/k_BT_P)$ in accordance with the description of the spectrum of rings. The canceling is due to the effect of the $\sinh^N(J/2k_BT_P)$ term which, however, is completely negligible in the thermodynamic limit $N \to \infty$. This means that the low-temperature behavior is not determined just by the low-lying states but may be governed by all the energy levels, especially when the level degeneracies vary as high powers of N. This important point of statistical mechanics is, of course, ignored in spin-wave theory, which bases an account of the finite temperature properties of a system on the lowest-lying excitations.

One must therefore exercise some discretion in interpreting energy gaps in connection with low-temperature thermodynamic behavior, and we shall see in the following subsection concerned with perturbation studies that the lowest-lying excitations of the Ising-Heisenberg system do not, in fact, determine an effective energy gap. This result is in accordance with the analytic results. From the preceding Ising example we may deduce some useful rules of thumb. If the degeneracy of the first excited level is $O(N)$, then the primary excitation gap is the same gap that determines the initial behavior of the thermal properties in the limit. On the other hand, if the levels are $O(N^2)$, as for the Ising rings, the effective gap is *half* the finite N primary gap. [In general, if the levels are $O(N^r)$, we may presume that the effective gap equals r^{-1} times the primary gap.] If the levels are only $O(1)$, the apparent primary gap has no relation to the effective limiting gap; this situation actually occurs for the Ising-Heisenberg linear ferromagnet.

One important point that emerges from the above considerations is that chains are likely to exhibit the effective energy gap whereas the rings exhibit the double gap. Hence, although periodic boundary conditions represent the standard approach, they also present a trap to the unwary, since the appropriate degeneracies necessary to estimate the effective gap, which may differ from the apparent gap, may be difficult to find in practice. Open-ended chains are thus seen to play a valuable independent role. This has now been observed to be the case in the linear Ising-Heisenberg *antiferromagnet* where the effective thermal gap has been estimated numerically,[40] and consequently demonstrated analytically,[37] to be half the gap calculated using periodic boundary conditions.[43]

B. Solution for one reversed spin

In terms of an Ising-type set of basis vectors $|i\rangle = |\uparrow\uparrow, \ldots, \uparrow\downarrow\uparrow, \ldots, \uparrow\uparrow\rangle$, where the ith spin is reversed ($i = 1, 2, \ldots, N$), the relevant subblock of the total Hamiltonian matrix for an N spin system is shown in Fig. 4.[50]

In the Heisenberg limit $\gamma = 1$, the tridiagonal, Toeplitz-type matrix of Fig. 4 is easily solved in terms of the eigenvector of Fig. 4(b). The matrix 4(a) operating on the trial eigenvector 4(b) for the internal states gives rise to the eigenvalue equation

$$E = 2J(1-\cos\theta) \quad . \tag{3.3}$$

The boundary conditions imposed by the end levels give the following condition on θ:

$$\sin N\theta = 0, \text{ i.e., } \theta = r\pi/N, \quad r = 0, 1, 2, \ldots, N-1 \quad . \tag{3.4}$$

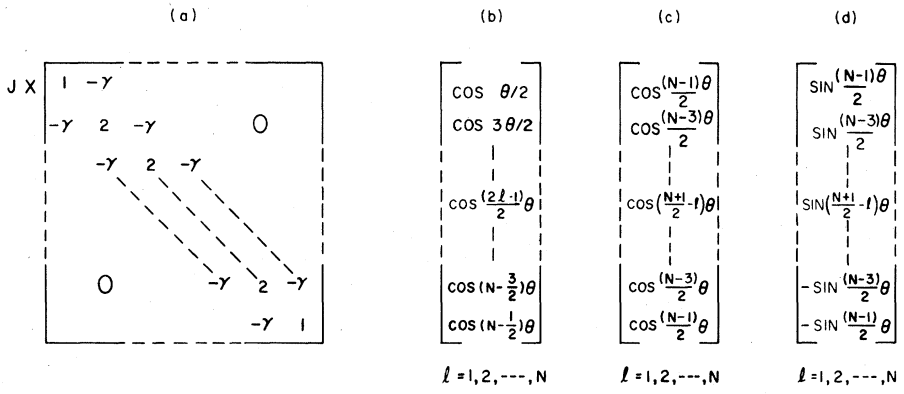

FIG. 4. (a) One overturned-spin matrix for an anisotropic Ising-Heisenberg linear chain with free-end boundary conditions. (b), (c), and (d) various eigenvectors for matrix (a). (See text.)

The solution, characterized by the wave vector $q_c = 9 = r\pi/N$, thus consists of a band of states between the energy limits $0 \leq E \leq 4J$. Let us compare the chain solution with the corresponding solution for rings, which is the well-known single-spin-wave solution. The matrix 4(a) now has simple cyclic form, and the eigenvalue equation is the same as Eq. (3.3). However, the corresponding wave vector for rings is given by

$$q_r = 2r\pi/N, \quad r = 0, 1, 2, \ldots, N-1 \ ; \qquad (3.5)$$

there are only half as many allowed energies with twice the energy interval.[51] In Fig. 5 the single-spin-wave dispersion curve as a function of wave vector q is shown as the dashed curve A for the finite system, $N = 8$. (Numerical calculations on rings up to $N = 12$ are now available, but the spectra are too complicated for simple display.) The open circles are the ring solutions and the solid circles, half of which coincide with the open circles, are the chain solutions.

For $\gamma < 1$ the solution for rings is modified only slightly. Equation (3.3) becomes

$$E = 2J(1 - \gamma \cos q_r) \ , \qquad (3.6)$$

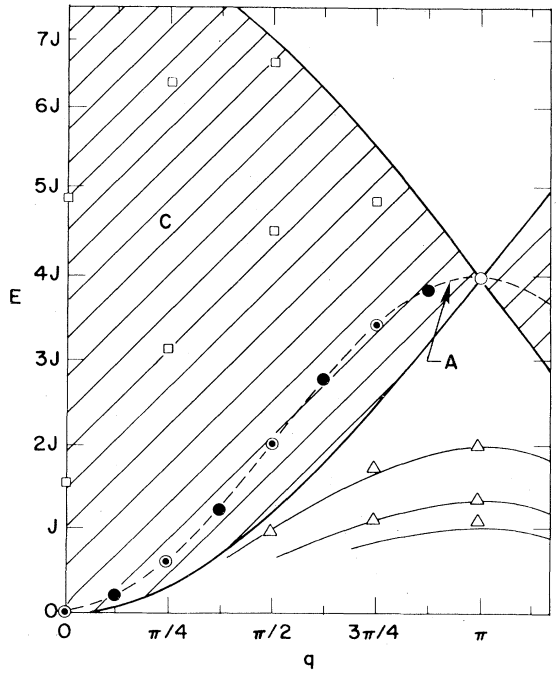

FIG. 5. Low-lying dispersion curves for the Heisenberg ferromagnet of 8 spins. Curve A is the single-spin-wave branch showing states corresponding to periodic (open circles) and free-end (filled circles) boundary conditions. The triangles denote bound states of total spin 0, 1, 2 in order of increasing energy. The shaded area C is the two-spin-wave continuum.

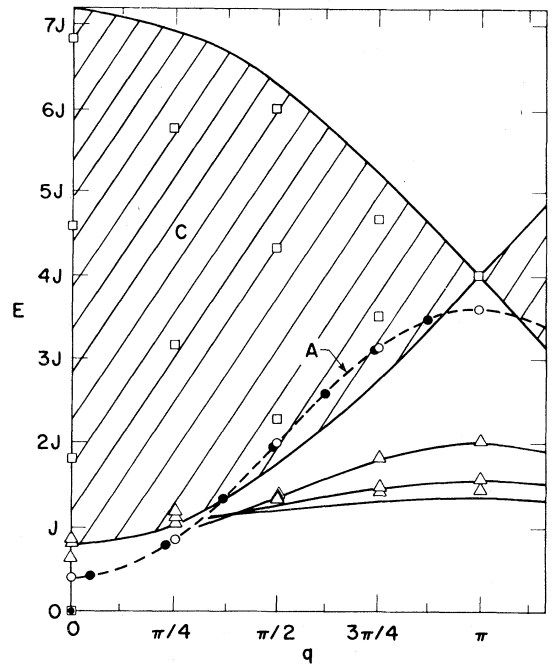

FIG. 6. Companion to Fig. 5, corresponding to anisotropy $\gamma = 0.8$. A is the single-spin-wave dispersion branch, C is the two-spin-wave continuum, and the triangles are bound states of 4, 3, 2 overturned spins in order of increasing energy.

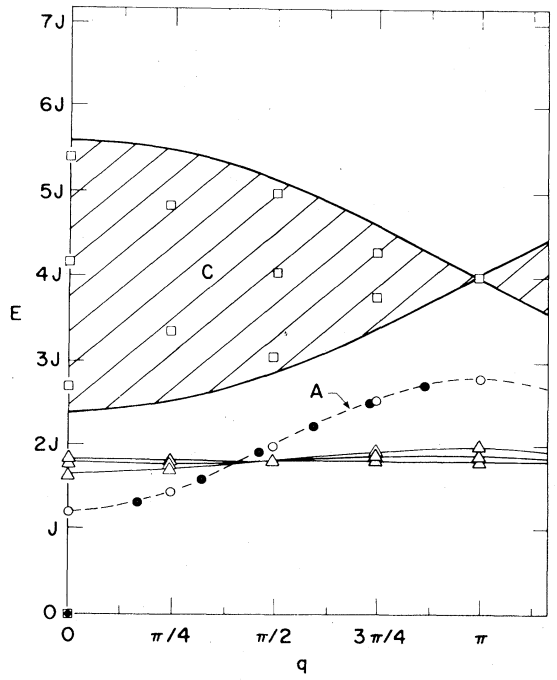

FIG. 7. Companion to Fig. 6, showing the distribution of spin wave and bound states for large anisotropy, $\gamma = 0.4$.

where the q_r are distributed as in Eq. (3.5) and the band limits are now

$$2J(1-\gamma) \leq E \leq 2J(1+\gamma) \quad . \tag{3.7}$$

In the case of chains the problem is still solvable by standard techniques, although the eigenvectors have a more complex form than that shown in Fig. 4(b). In fact, there are two classes of solution corresponding to eigenvectors 4(c) and 4(d). The overall solution shows a striking change from the Heisenberg limit solution [and also the periodic (ring) solution for all γ] in that two states (bound states) are now split off the band.[52] The remaining $(N-2)$ states have the band solution of Eq. (3.6), although the θ distribution is more complicated than for $\gamma = 1$. The allowed solutions for θ now divide into two classes, A and B, corresponding to eigenvectors 4(c) and 4(d), respectively:

$$\gamma\cos\theta - 1 = \begin{cases} \gamma \tan(N-1)\tfrac{1}{2}\theta \sin\theta & (3.8) \\ -\gamma\cos(N-1)\tfrac{1}{2}\theta\sin\theta. & (3.9) \end{cases}$$

In Figs. 6 and 7 the single spin-wave dispersion curves are again shown as curve A, and again the open circles are the periodic and the dark circles are the free-ended chain states. Notice that, as γ decreases, the chain states are increasingly displaced towards lower q with reference to their $\gamma = 1$ locations.

For the two bound states, arising from the end levels of matrix 4(a), simple perturbation theory gives the result

$$E = J(1-\gamma^2) \quad . \tag{3.10}$$

Letting $\theta \to i\phi$, it is easy to show that solution classes A and B [Eqs. (3.8) and (3.9)] each yield a single bound state in the limit $N \to \infty$ with the eigenvalue $E_{A,B} = J(1-\gamma^2)$. Hence, perturbation theory gives the exact solution for all γ in the limit $N \to \infty$.

Therefore, taking account of the $\pm S^z$ degeneracy, a total of *four* bound states split off the single-spin-wave continuum, as shown in Fig. 8. For $0 \leq \gamma < 1$ they are the lowest-lying excitations of the Ising-Heisenberg linear chain.

C. Perturbation studies for two and more reversed spins

For two and more reversed spins an exact solution is no longer possible for free-end boundary conditions; thus we shall use perturbation theory. All Hamiltonian submatrices for two and more overturned spins have the simplified form shown in Fig. 9.[53] Second-order perturbation theory for the end levels of block (α), which form the lowest-lying ferromagnetic levels of the problem, gives

$$E = J(1-\tfrac{1}{2}\gamma^2) \quad . \tag{3.11}$$

Since we must consider states of positive and negative S^z, there will be $2(N-3)$ such special, end-level, bound states, which are degenerate in second-order perturbation theory with energy $J(1-\frac{1}{2}\gamma^2)$. Numerical studies show that the degeneracy of the $2(N-3)$ levels is split slightly for finite N and γ near 1. However, it can be shown that the levels become degenerate in the Heisenberg limit as $N \to \infty$ [since the energy spread is $O(1/N^2)$]. Therefore, since they are degenerate in the Ising limit and in the

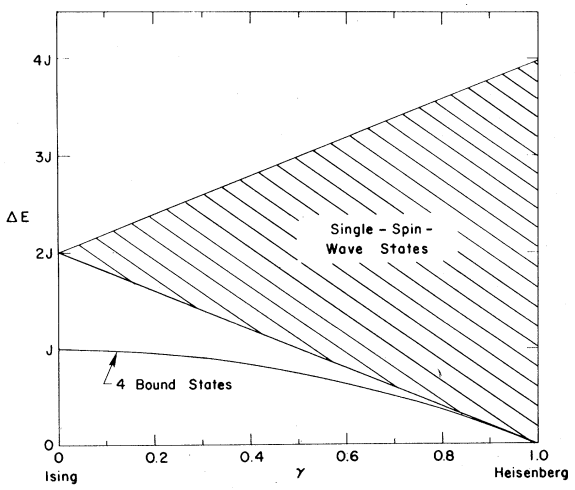

FIG. 8. Exact one overturned-spin solution for free-end chains. Four bound states are split off (lie below) the band because of the free-end perturbation.

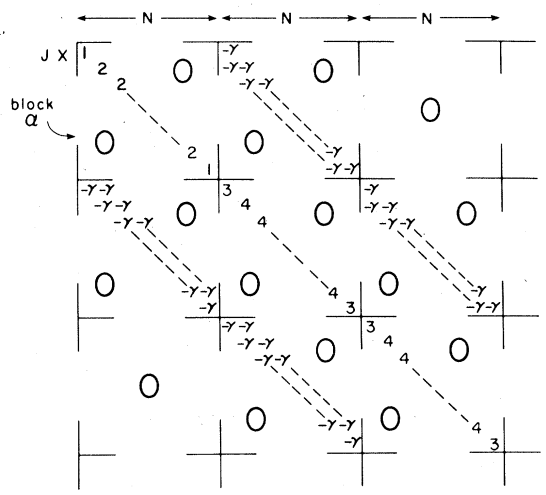

FIG. 9. Hamiltonian matrix for free-end chain systems for general anisotropy and two overturned spins (schematic).

Heisenberg limit as $N \to \infty$, it is very plausible that for $N \to \infty$ the levels remain degenerate for all γ.[54]

In Fig. 10 the dashed curve (a) is the $N \to \infty$ extrapolation of the chain bound-state levels for two and more overturned spins; also shown are the finite N curves for $N = 4$, 6, and 8 from which the extrapolation was made. It may be noted that dashed curve (d) corresponds to the four degenerate chain bound states for one overturned spin, discussed in subsection III B. Although curve (d) lies lower than curve (a), it contains only four states as opposed to $O(N)$ states, and the states of curve (d) are, therefore, thermodynamically insignificant in comparison with those of curve (a), according to the arguments of subsection III A.

For two and more overturned spins bound states appear in the ring solutions as well as in the chain solutions. Ring bound states are illustrated as open triangles in Figs. 5, 6, and 7. It is notable in Fig. 7 ($\gamma = 0.4$) that the bound states for each value of q are almost degenerate and the energy spread of the bound-state band is very small. Hence, in the $N \to \infty$ limit we expect $O(N^2)$ bound states in a very narrow band. The $N \to \infty$ bound-state curve for rings is shown as curve (b) in Fig. 10. Within the accuracy of extrapolation, curve (b) is just twice curve (a) for chains. However, since there are $O(N^2)$ states in curve (b) compared with $O(N)$ for curve (a), the *effective gap* for the bound states of curve (b) is identical with curve (a), in accordance with the arguments of subsection III A. This, of course, simply implies that chains and rings are equivalent in terms of limiting, $N \to \infty$, spectral excitations, as we would expect.

Having established that the dominant bound-state excitations are given by curve (a) of Fig. 10 and that the corresponding effective energy gap is the difference between curve (a) and the ferromagnetic ground-state energy ($E/J = 0$ for all γ), we must now consider other types of excitation. In Fig. 10 we show the lower edge of the single-spin-wave continuum as a function of γ [curve (c)]. For $\gamma \lesssim 0.6$ the spin-wave continuum is appreciably higher in energy than the dominant bound-state curve (a). Therefore, we expect the dominant spectral excitations to correspond to bound states, and the spectral energy gap to be given by $\Delta E = J(1 - \frac{1}{2}\gamma^2)$ in second-order perturbation theory. Although this perturbation expression differs from the exact result, $\Delta E = J(1-\gamma^2)^{1/2}$, actual numerical differences are slight in the range $0 \leq \gamma < 0.6$.[55] At this point it might also be informative to compare our bound-state gap extrapolations [curve (a) of Fig. 10] with the exact results. This is done in Fig. 11 and the agreement is gratifying. In Fig. 11 we show also the exact result[43] for the antiferromagnet energy gap.

Let us now consider the other end of the anisotropy range, approaching $\gamma = 1$. The lower edge of the single-spin-wave continuum [curve (c) in Fig. 10] *crosses* the extrapolated bound-state curve (a) in the vicinity of $\gamma = 0.6$, and for $0.6 \lesssim \gamma < 1$ the spin-wave continuum states lie lower than the bound states. It seems persuasive to argue that the anisotropic energy gap is therefore dominated by the spin-wave states, but we must be careful that there are enough such states. The single-spin-wave band contains $O(N)$ states spread over the whole energy range $2J(1 \pm \gamma)$, i.e., over $\Delta E = 4J\gamma$, in comparison with $O(N)$ states in the bound-state curve (a) of Fig. 10. In Fig. 5 a two-spin-wave continuum is shown as the shaded area C for the Heisenberg limit. In this limit each state in the continuum (shown as an open square for $N = 8$) is a multiplet of total spin $S = N/2 - 2$ and

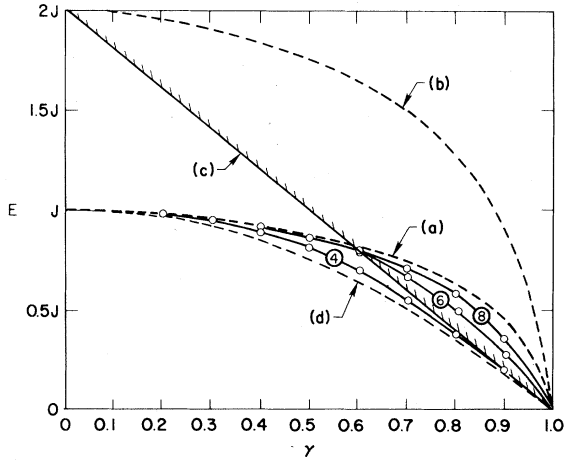

FIG. 10. Low-lying excitations for the Ising-Heisenberg ferromagnet as a function of anisotropy γ. (a) is the extrapolated bound-state curve for chains. Curves from which the extrapolation was performed are shown for $N = 4$, 6, and 8. Curve (b) is the extrapolated bound-state curve for rings. (c) is the lower edge of the single-spin-wave band. (d) is a curve containing 4 one overturned-spin bound states, and has negligible weight in the thermodynamic limit.

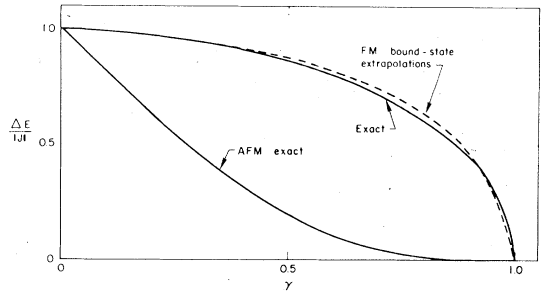

FIG. 11. Comparison of exact result and finite N extrapolations for the anisotropic, Ising-Heisenberg, ferromagnetic, bound-state energy gap. The exact result for the antiferromagnetic energy gap is shown for comparison.

degeneracy $2(N/2-2)+1=N-3$. The continuum is bounded by the curves $4J(1\pm\cos\frac{1}{2}q)$ (Ref. 56) and, therefore, has an energy range $\Delta E=8J\cos\frac{1}{2}q$. It encloses the single-spin-wave continuum, curve A, and is evidently codominant with it in terms of spectral excitations. In Fig. 6, for $\gamma=0.8$, the role of the two-spin-wave continuum C is not so clear. For $0\leq\gamma\leq 1$ the continuum is bounded by the curves $4J(1\pm\gamma\cos\frac{1}{2}q)$ with an energy spread of $\Delta E=8\gamma J\cos\frac{1}{2}q$. The single-spin-wave curve A no longer lies wholly inside C. In particular, in the lowest-energy region at small q, the single-spin-wave curve is lower in energy (by a factor of $\frac{1}{2}$). However, there are $O(N^2)$ states in continuum C as opposed to $O(N)$ states in curve A, and, hence, both classes of spin-wave states remain codominant, even for $q\to 0$. In fact, by the arguments of subsection III A the C states are always codominant with the single-spin-wave A states for all γ. In the case of Fig. 7, corresponding to $\gamma=0.4$, the single-spin-wave continuum lies entirely below the two-spin-wave continuum. However, in this anisotropy region both are dominated by the bound states.

We therefore have an explanation of the analytic result that at $\gamma=0.6$ the character of the thermal, ferromagnetic, excitation energy gap changes. For $\gamma>0.6$ the spin-wave states dominate the bound states, giving an effective energy gap $\Delta E=J(1-\gamma)$ in accordance with the analytic result. This effect is illustrated in Fig. 12, which again includes the antiferromagnetic energy gap for comparison.

To summarize, the various competing classes of states are shown schematically in Fig. 13 as a function of γ. The lowest-lying curve of all, curve (a), represents the four one overturned-spin bound states, and, therefore, this curve is not significant in the thermodynamic limit. The region B comprises the bound states of 2, 3, . . . , $N/2$ overturned spins. The $O(N^2)$ degeneracy of the states in this region

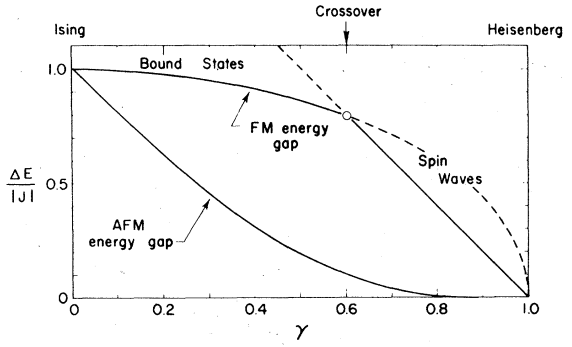

FIG. 12. Comparison to Fig. 11, showing the crossover of bound-state-dominated and spin-wave-dominated regions at $\gamma=0.6$ $(\Delta=\frac{5}{3})$.

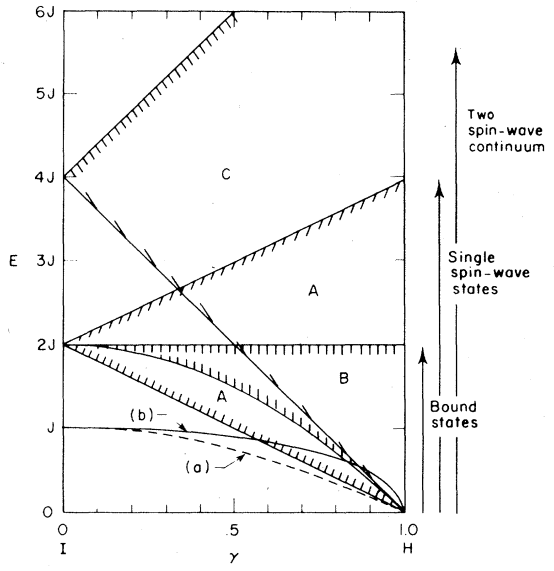

FIG. 13. Overall display of the spectral excitations of the anisotropic Ising-Heisenberg ferromagnet as a function of anisotropy in zero field. (See text.)

gives rise to an effective bound-state dispersion curve [curve (b)] lower in energy. This curve would be obtained directly by using free end rather than periodic boundary conditions. Region A contains $O(N)$ single spin-wave states, which are codominant with the two-spin-wave states of region C. Although region C lies higher in energy than region A, the C states are $O(N^2)$ and, therefore, effectively reinforce the states of region A.

IV. CONCLUSION

Important analytic results have been obtained for the linear Ising-Heisenberg model in a parameter range which has hitherto resisted such calculations. In particular, an expression has been obtained for the zero-field thermal excitation energy gap for the Ising-Heisenberg linear ferromagnet. This expression is unusual in that it changes its form at an intermediate value of a variable anisotropy parameter. This special value does not correspond to any symmetry change in the Hamiltonian, but *is* associated with an important change in the physical significance of the results. For anisotropy greater than the special value, the dominant excitations correspond to bound spin complexes (localized magnons) of 2, 3, . . . , $N/2$ reversed spins. For anisotropy less than the special value, the dominant excitations are spin waves. However, it turns out that this effective excitation gap applies only to thermal derivatives of the free energy, e.g., the specific heat. The susceptibility is

governed by the magnetic excitation gap, corresponding to the bound spin complexes for the whole anistropy range $0 \leq \gamma < 1$. Thermal and magnetic gaps coincide for anisotropy less than the special value, but they differ for anisotropy greater than the special value.

Numerical studies show that the Ising-Heisenberg ferromagnetic excitation spectrum is unusually complicated with different classes of states competing for dominance. A careful examination of finite-N linear systems, however, supports the analytic results. The numerical arguments developed should be valuable for problems where an analytic result is not available.

The ferromagnetic limit, $\gamma = 1$, is an especially difficult problem, which at present defies both intuition and analytic attack. Previous work of Wortis and others[57] has demonstrated the existence of low-lying bound complexes in the linear Heisenberg ferromagnet, and the validity of simple spin-wave theory is again in considerable doubt. Finite-chain excitation spectra show clearly the low-lying bound states of Bethe[33] and Wortis[57] and also higher excitations which are not in the spin-wave class. These excitations may be higher-order excited bound states or a missed spin wave or bound type. They may be numerous enough to influence at least some of the thermodynamic properties.[40] It is interesting to view this situation in the light of our present knowledge of the low-lying excitations in the Heisenberg-XY region.[58] No bound states occur for either the ferro- or antiferromagnetic XY limit. Bound states of two and more reversed spins develop successively as one approaches the ferromagnetic Heisenberg limit from the XY direction. The ferromagnetic Heisenberg-XY system is known[58] to have no gap in the excitation spectrum. It is nevertheless tempting to speculate whether unusual effects may show up in the susceptibility or specific heat at some intermediate point between Heisenberg and XY limits when the bound states become sufficiently numerous. In this connection we recall Takahashi's work on the $H_0 = 0$ XYZ model,[48] previously discussed in subsection II C. For the XYZ model in zero field, close to the ferromagnetic Heisenberg-XY limit, a gap occurs in the excitation spectrum which has similar crossover character to the ferromagnetic Ising-Heisenberg gap. Takahashi does not extend his complete analysis to the Heisenberg-XY line, but the situation is suggestive that unusual behavior may be observed in this limit and further investigation would be interesting.

These results should have an important bearing on the quantum soliton problem in the linear-chain ferromagnet.[59] Now that the class of experimental ferromagnets has been enlarged, these results should be susceptible to experimental examination.

ACKNOWLEDGMENTS

One of us (J.C.B.) would like to thank John F. Nagle for clarifying discussions on the significance of level degeneracies and to acknowledge the early contributions of Michael E. Fisher. J.C.B. would like to thank Brookhaven National Laboratory for the hospitality of its summer visitor's program, during which some of this work was carried out. This work was supported in part by the U.S. Department of Energy, Contracts No. W-7405-ENG-36 and No. EY-76-C-02-0016, and the U.S. National Science Foundation, Grant No. DMR77-24136. One of us (J.C.B.) would like to acknowledge the support of the Bunting Institute, Radcliffe College, Cambridge, Massachusetts.

[1] J. C. Bonner, J. Appl. Phys. 49, 1299 (1978).
[2] C. K. Lai, Phys. Rev. A 8, 2567 (1973).
[3] M. Takahashi, Prog. Theor. Phys. 46, 1388 (1971).
[4] H. G. Vaidya and C. A. Tracy, Phys. Rev. Lett. 42, 3 (1979); 43, 1540 (1979); J. Math. Phys. 20, 2291 (1979).
[5] M. Takahashi, Prog. Theor. Phys. 43, 1619 (1970); 52, 103 (1974).
[6] A. Luther and I. Peschel, Phys. Rev. B 12, 3908 (1975).
[7] D. C. Mattis and E. Lieb, J. Math. Phys. 6, 304 (1965).
[8] H. Gutfreund and M. Schick, Phys. Rev. 168, 418 (1968).
[9] A. Luther and V. J. Emery, Phys. Rev. Lett. 33, 589 (1974).
[10] S.-T. Chui and P. A. Lee, Phys. Rev. Lett. 35, 315 (1975).
[11] V. J. Emery, A. Luther, and I. Peschel, Phys. Rev. B 13, 1272 (1976).
[12] A. Luther, Phys. Rev. B 15, 403 (1977).
[13] V. J. Emery, in *Highly Conducting One-Dimensional Solids*, edited by J. T. Devreese *et al.* (Plenum, New York, 1979), Chap. 6.
[14] B. Sutherland, Phys. Rev. Lett. 35, 185 (1975); 34, 1083 (1975).
[15] B. Sutherland, Phys. Rev. B 12, 3795 (1975).
[16] V. J. Emery, Phys. Rev. B 14, 2989 (1976).
[17] M. Fowler, in *Organic Conductors and Semiconductors: Proceedings of the International Conference*, edited by L. Pál *et al.* (Springer-Verlag, Berlin, 1977), p. 51.
[18] M. Fowler, Phys. Rev. B 17, 2989 (1978).
[19] M. Fowler and M. W. Puga, Phys. Rev. B 18, 421 (1978).
[20] M. Suzuki, Prog. Theor. Phys. 46, 1337 (1971).
[21] M. Suzuki, Prog. Theor. Phys. 56, 1454 (1976).
[22] M. Barma and B. S. Shastry, Phys. Rev. B 18, 3351 (1978).
[23] N. Ishimura and H. Shiba, Prog. Theor. Phys. 57, 1862 (1977).
[24] M. W. Puga, Phys. Rev. Lett. 42, 405 (1979).
[25] G. Müller, H. Beck, and J. C. Bonner, Phys. Rev. Lett. 43, 75 (1979).
[26] M. Fowler and M. W. Puga, Phys. Rev. B 19, 5906 (1979).
[27] H. Gutfreund and R. A. Klemm, Phys. Rev. B 14, 1073 (1976).
[28] V. J. Emery, Phys. Rev. Lett. 37, 107 (1976).

[29]H. Bergknoff and H. B. Thacker, Phys. Rev. Lett. 42, 135 (1979).
[30]L. D. Fadeev (unpublished).
[31]A. Luther, Phys. Rev. B 14, 2153 (1976).
[32]B. Sutherland, Rocky Mount. J. Math. 8, 413 (1978).
[33]H. A. Bethe, Z. Phys. 71, 205 (1931).
[34]L. Hulthén, Ark. Mat. Astron. Fys. 26A, 1 (1938).
[35]C. N. Yang and C. P. Yang, Phys. Rev. 150, 321 (1966); 150, 327 (1966); 151, 258 (1966).
[36]M. Gaudin, Phys. Rev. Lett. 26, 1301 (1971).
[37]J. D. Johnson and B. M. McCoy, Phys. Rev. A 6, 1613 (1972).
[38]J. D. Johnson, Phys. Rev. A 9, 1743 (1974).
[39]J. C. Bonner and M. E. Fisher, Phys. Rev. 135, A640 (1964).
[40]J. C. Bonner, Ph.D. thesis (University of London, 1968 unpublished).
[41]J. D. Johnson, B. M. McCoy, and C. K. Lai, Phys. Lett. A 38, 143 (1972); M. Takahashi and M. Suzuki, Phys. Lett. A 41, 81 (1972).
[42]At $\gamma = 1$ (isotropic Heisenberg limit) the gap vanishes and the $T = 0$ singularities are governed by power laws. This result is not in conflict with smoothness universality because the symmetry of the Hamiltonian changes at this special point.
[43]J. des Cloizeaux and M. Gaudin, J. Math. Phys. 7, 1384 (1966). See corrected excitations in Ref. 37.
[44]J. B. Torrance, Jr., and M. Tinkham, Phys. Rev. 187, 595 (1969).
[45]C. P. Landee and R. D. Willett, Phys. Rev. Lett. 43, 463 (1979).
[46]L. R. Walker, Phys. Rev. 116, 1089 (1959).
[47]*Higher Transcendental Functions,* edited by A. Erdelyi *et al.* (McGraw-Hill, New York, 1953).
[48]M. Takahashi, Prog. Theor. Phys. 50, 1519 (1973).
[49]K. Huang, *Statistical Mechanics* (Wiley, New York, 1963).
[50]Energies are defined relative to the (twofold degenerate, all spins aligned) ferromagnetic Ising-Heisenberg ground state. With the Hamiltonian defined as in Eq. (1.1), the ground state is zero for all γ.
[51]The situation is, of course, analogous to the case of vibrating linear systems with fixed and periodic boundary conditions.
[52]*One* bound state always occurs for any finite N and γ. The occurrence of the second bound state is determined by N and γ, and is favored by large N and γ near 1. Two bound states appear in the limit $N \to \infty$ for all $\gamma < 1$.
[53]The actual matrices are rather more complicated than is suggested by Fig. 9, but give identical results as far as perturbations of the two lowest-lying end levels are concerned.
[54]Our perturbation expression, Eq. (3.11), is equivalent to that obtained by J. B. Torrance, Jr., and M. Tinkham, Phys. Rev. 187, 587 (1969) by an Ising basis function method. See also Ref. 40.
[55]Preliminary results have been presented in two talks, J. D. Johnson and J. C. Bonner, J. Appl. Phys. 49, 1334 (1978); J. C. Bonner, H. W. J. Blöte, and J. D. Johnson, J. Phys. (Paris) 39, C6-710 (1978). However, in these talks the exact result $\Delta E = J(1-\gamma^2)^{1/2}$ was not present, but instead the small-γ expansion $\Delta E \simeq J(1-\frac{1}{2}\gamma^2)$ was given. The perturbation expansion is actually a very good approximation to the exact result over the anisotropy range of interest.
[56]See discussion in Ref. 39.
[57]M. Wortis, Phys. Rev. 132, 85 (1963).
[58]J. D. Johnson, S. Krinsky, and B. M. McCoy, Phys. Rev. A 8, 2526 (1973).
[59]P. P. Kulish and E. K. Sklyanin, Phys. Lett. A 70, 461 (1979).